Coalescence and Reactivity of Gold−Silver Bimetallic Clusters in Cyanide Solution

C. de Cointet, J. Khatouri, M. Mostafavi, and J. Belloni*

Laboratoire de Physico-Chimie des Rayonnements, Associé au CNRS, Bâtiment 350, Université Paris-Sud, 91405 Orsay, France

Received: October 28, 1996; In Final Form: February 27, 1997[⊗]

Pulse radiolysis of mixed solutions of two monovalent metals, $Ag^{I}(CN)_2^-$ and $Au^{I}(CN)_2^-$, has permitted the dynamics of the alloying process between gold and silver and the reactions of the alloyed cluster to be followed from the nanosecond to the second time range. The pulse induces simultaneous reduction of the ions into silver and gold atoms. Then, through coalescence and association with excess ions, homologue or different, these coexisting atoms give rise to transient bimetallic alloyed clusters. However, in the interval 2−20 s the clusters are enriched in silver at the expense of gold, the process being assigned to a slow intermetal electron transfer from gold atoms (less noble in the presence of CN^-) to silver ions adsorbed on clusters. In the presence of the electron acceptor/donor couple $MV^{2+}/MV^{\bullet+}$, gold atoms generated in monometallic $KAu(CN)_2$ solutions act as an electron relay and readily transfer electrons to MV^{2+} as they are oxidized. In contrast, when silver and gold atoms are generated simultaneously, the transient bimetallic clusters that form behave as a catalytic electron acceptor toward $MV^{\bullet+}$ above a critical nuclearity, as for pure silver clusters, and grow as large alloyed particles. It is concluded that even in low proportions, silver increases the redox potential of mixed clusters relative to pure gold clusters in the presence of cyanide.

Introduction

Bimetallic clusters are of very high interest in catalysis.[1] In the field of photographic processes for example, empirical results have long demonstrated the role of gold as a catalytic sensitizer for the development of silver clusters in exposed emulsions. The dynamics of the metal ion reduction and of the growth and reaction of clusters in solution with an electron donor have already been studied by the pulse radiolysis technique for different systems, mostly monometallic.[2−5] Early steps of the reduction in mixed systems such as Ag^+/Ni^{2+},[6] Ag^+/Tl^+,[7] Ag^+/Cd^{2+},[8] and Ag^+/Co^{2+} [8] have been observed less often by pulse radiolysis. The aim of this work is to extend this type of investigation to a couple of metal ions in order to follow by time-resolved techniques the progressive building and the reactive properties of the bimetallic clusters. Particularly, we intend to examine whether the metals are intimately alloyed in the cluster[5,9,10] or successively reduced so that the metals are segregated in a core−shell structure.[10−12]

The system selected for the study is the couple $Ag(CN)_2^-/Au(CN)_2^-$, where both metal cations are monovalent and are complexed with the same ligand. In the first part[4] of this study, clusters formed in the radiation-induced reduction of $Ag(CN)_2^-$ have been thoroughly examined. In this second part, our purpose is to compare the effect of the perturbation introduced by the simultaneous presence of the $Au(CN)_2^-$ ions on the coalescence and the electron transfer kinetics. The dynamics of $Au(CN)_2^-$ reduction and of monometallic cluster formation have already been investigated.[13] In addition to the coalescence of the mixed cluster, its reactivity with a reference redox couple will be compared with that of each of the monometallic clusters under the same conditions.[4]

Experimental Section

All reagents were pure chemicals: gold and silver salts, $KAu(CN)_2$, and $KAg(CN)_2$, were from Comptoir Lyon Alemand Louyot (therefore we did not have to add CN^- ions to prepare the cyanide complexes). The chemicals 2-propanol, sodium formate, and acetone were from Prolabo and methyl viologen chloride was from Aldrich. Mixed solutions of gold and silver cyanide were stable for hours with no change in the UV spectrum for the specific bands of the $Au(CN)_2^-$ complex at 232 and 242 nm. Solutions were thoroughly deaerated by flushing nitrogen gas or by degassing under vacuum.

γ-Irradiation facilities (dose-rate 10−30 kGy h^{-1}) and pulse radiolysis equipment (dose per pulse from 0.15 to 1.2 kGy) have already been described.[4] The ions Ag^I and Au^I are reduced by hydrated electrons and $OH^\bullet$ and $H^\bullet$ radicals are scavenged by 2-propanol or 0.2 mol L^{-1} $NaHCO_2$ and replaced by $(CH_3)_2C^\bullet OH$ or $CO_2^{\bullet-}$ radicals with strong reducing properties.

Results and Discussion

$Au(CN)_2^-$ Solutions. Following the procedures of previous experiments,[4] $KAu(CN)_2$ solutions were irradiated for comparison in the absence and presence of the methyl viologen couple used as a redox indicator.

Gold Solutions without MV^{2+}. The solution contains only the precursor $KAu(CN)_2$ and 2-propanol. By reaction with solvated electrons generated by the pulse, the complexed atoms $Au(CN)_2^{2-}$ are obtained ($\lambda_{max} = 400$ nm and $\epsilon_{400} = 10^3$ L mol^{-1} cm^{-1}).[13]

$$Au(CN)_2^- + e_{aq}^- \rightarrow Au(CN)_2^{2-} \qquad (1)$$

The pseudo-first-order rate constant of the electron decay at 700 nm is proportional to the initial concentration of the precursor salt in the interval $(0.5-5) \times 10^{-3}$ mol L^{-1}. The bimolecular rate constant of reaction 1 is found to be close to the published values, $k_1 = 8 \times 10^9$ L mol^{-1} s^{-1} [14] and 1.1×10^{10} L mol^{-1} s^{-1}.[13] In Figure 1 the formation of gold oligomers and finally at long time of gold particles Au_{n,CN^-} (where the nuclearity n refers to the number of atoms effectively reduced in the cluster) is observed at 520 nm. During the growth, complexed gold atoms coalesce slowly, yielding the

[⊗] Abstract published in *Advance ACS Abstracts,* April 1, 1997.

S1089-5647(96)03344-5 CCC: $14.00

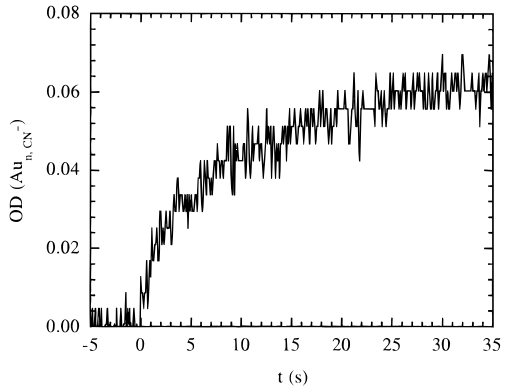

Figure 1. Growth kinetics of gold clusters in cyanide solution at $\lambda = 520$ nm. $[KAu(CN)_2] = 2 \times 10^{-3}$ mol L^{-1}; [iPrOH] $= 2 \times 10^{-1}$ mol L^{-1}.

clusters associated with complex ions $Au_{n+x}{}^{x+}{}_{,CN^-}$. Infact the spectra of gold oligomers or ultrasmall clusters do not exhibit any maximum but absorb below 400 nm.[13] When the nuclearity increases, the absorption spectrum increases in intensity and extends above 550 nm. Finally, the plasmon band of nanometric clusters appears with a maximum located at 520 nm.[15,16]

The extinction coefficient of Au_{n,CN^-} increases with the nuclearity, and hence the optical density increases as the growth proceeds. Complete reduction of a millimolar $Au(CN)_2^-$ solution (initial pH = 5.7) by γ-irradiation leads to the classical absorption spectrum of gold clusters and allowed us to determine their extinction coefficient under these conditions: $\epsilon(Au_{n,CN^-})_{520} = 4000$ L mol^{-1} cm^{-1}. From the slope of the linear absorbance increase with dose and from $\epsilon(Au_{n,CN^-})_{520}$ we derive the reduction radiolytic yield G_{red}, which is low ($G = 1.2$ atoms per 100 eV) compared to the total yield of reducing radicals $G_{red} = 6$. In the previous study,[13] performed at a dose rate much lower than in the present work, the yield (also less than 6) is somewhat higher than in this case due to a more efficient radical scavenging in competition with the slow radical−radical recombination. When acetone is added to the $KAu(CN)_2$ and 2-propanol solution, in order to replace all radiolytic species by $(CH_3)_2C^{\bullet}OH$ radicals, we do not observe any gold formation. In fact, the reaction between hydroxy propyl radicals and the cyano complex of gold is unlikely due to the strongly negative redox potential of the gold couple involved in reaction 1. In the case of cyano−silver the same phenomenon has been already predicted from calculation[17] and experimentally observed.[18] This suggests that the redox potential of the cyano complex of the zero-valent gold monomer is quite negative: $E°(Au(CN)_2^-/Au°\text{-}(CN)_2^{2-}) < E°((CH_3)_2C^{\bullet}OH)/(CH_3)_2CHOH))$. Actually, the zero-valent monomer of gold should be complexed by CN^-, as demonstrated for $Ag(CN)_2^{2-}$.[12,17,18] The gold clusters are readily oxidized by oxygen when in contact with air. This observation is also coherent with the negative electrochemical potential of the gold electrode in cyanide solutions $E°(Au\text{-}(CN)_2^-/Au_{met}+2CN^-) = -0.6$ V_{NHE}.[19]

It is clear from the signal in Figure 1 that the absorbance increase is extremely slow, as the plateau is reached only at 30 s (compared to 20 ms for Ag_{n,CN^-}[4]). The increase is due to the coalescence process and to an increase with the nuclearity of the extinction coefficent per atom. We consider that the delay corresponds to the time necessary for the full development of the surface plasmon spectrum when ϵ becomes independent of the nuclearity. Previous works[15,16] in chloride medium have shown that this occurs for gold clusters of 1−2 nm diameter (about a few tens of atoms) only. We may therefore derive

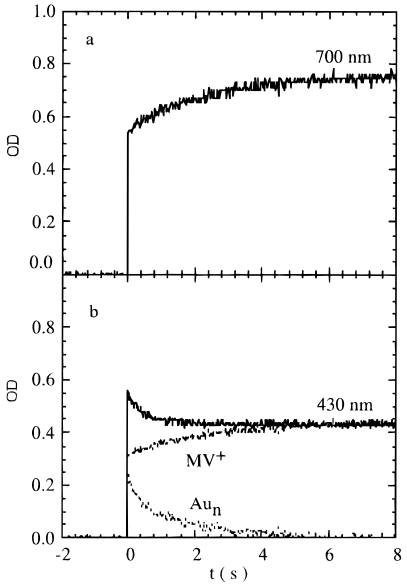

Figure 2. Correlated signals at $\lambda = 700$ nm (a) and $\lambda = 430$ nm (b) with a single pulse. $[KAu(CN)_2] = 5 \times 10^{-4}$ mol L^{-1}; $[MV^{2+}] = 5 \times 10^{-4}$ mol L^{-1}; $[NaHCO_2] = 2 \times 10^{-1}$ mol L^{-1}.

from the signal of Figure 1 and from the growth kinetics model[20] an approximate value of the mean coalescence rate constant k_d. The k_d value is around 10^4 L mol^{-1} s^{-1} for gold clusters in the presence of cyanide, instead of $(6 \pm 2) \times 10^6$ L mol^{-1} s^{-1} for silver. This result emphasizes the exceptional slowness of the growth process, probably because of the strong complexation of the gold with CN^-. The equilibrium constant for the complexation for the Au^I is indeed[21] $[Au(CN)_2^-]/[Au^+] \times [CN^-]^2 = 2 \times 10^{38}$ (L mol^{-1})^2 instead of 2.7×10^{20} (L mol^{-1})^2 for silver.[22] Note that the coalescence could even be completely stopped, such as for silver clusters with $n \geq 4$ when the ligand is polyacrylate[23].

Gold Solutions in the Presence of MV^{2+}. The same redox reference $MV^{2+}/MV^{\bullet+}$ has been selected as for the preceding study.[4] Due to the overlap of the Au_n spectrum with $MV^{\bullet+}$ bands, the Au_n growth is better observed at 420 nm, near the minimum of the $MV^{\bullet+}$ absorption spectrum, and the $MV^{\bullet+}$ decay at 700 nm ($\epsilon_{700}(MV^{\bullet+}) = 3460$ L mol^{-1} cm^{-1}). Moreover, the signal may be compared with that of pure silver[4] or that of the silver−gold mixture (below). The two precursors contained in the solution to be irradiated ($[KAu(CN)_2] = 5 \times 10^{-4}$ mol L^{-1} and $[MV^{2+}] = 5 \times 10^{-4}$ mol L^{-1}) are stable in the presence of each other.

After the pulse, the strongly reducing species e_{aq}^- readily reacts with both precursors, $Au(CN)_2^-$ and MV^{2+}, yielding metal atoms and the potential indicator $MV^{\bullet+}$. Alcohol radicals are scavenged by MV^{2+} exclusively. Postulating an increase of the redox potential of Au_n with n, the potential is shifted positively during the coalescence from the initial atoms to clusters. If they could grow enough to reach a potential higher than that of the donor, the electron transfer would occur from $MV^{\bullet+}$ to $Au^+{}_{n,CN^-}$. As in the preceding study with $Ag(CN)_2^-$,[4] we should observe the decay of the donor after a critical time and, simultaneously, the growth of the clusters.[6]

In fact, the signal in Figure 2a corresponding to $MV^{\bullet+}$ does increase at 700 nm instead of decaying as in the $MV^{\bullet+}$/silver system. The signal at 420 nm is too intense as compared to OD at 700 nm to belong only to $MV^{\bullet+}$: it is also due partly to Au_{n,CN^-}. It decreases (Figure 2b) while on the same time scale the absorbance OD_{700} correlatively increases. The absorbance at 420 nm can indeed be decomposed into two components: an increase of $MV^{\bullet+}$, which may be derived from the 700 nm

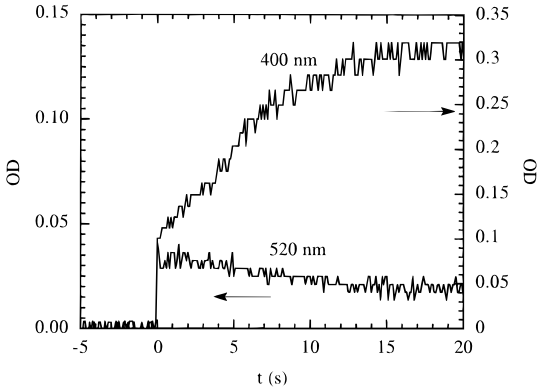

Figure 3. Correlated signals at $\lambda = 400$ nm and $\lambda = 520$ nm with a single pulse. $[KAg(CN)_2] = 5 \times 10^{-4}$ mol L^{-1}; $[KAu(CN)_2] = 5 \times 10^{-4}$ mol L^{-1}; [iPrOH] $= 2 \times 10^{-1}$ mol L^{-1}.

absorbance due only to $MV^{\bullet+}$, and a decrease down to zero assigned to Au_{n,CN^-}.

$$OD_{420} = OD_{420}(Au_{n,CN^-}) + OD_{420}(MV^{\bullet+}) = OD_{420}(Au_{n,CN^-}) + OD_{700}(MV^{\bullet+}) \times \epsilon_{420}(MV^{\bullet+})/\epsilon_{700}(MV^{\bullet+}) \quad (2)$$

The contribution of zero-valent gold corresponds to the difference between the experimental signal and $OD_{420}(MV^{\bullet+})$ (Figure 2b).

These results strongly suggest that the electron transfer from $MV^{\bullet+}$ to gold clusters does not occur, and in contrast electrons are transferred from gold clusters to MV^{2+}, which oxidizes the small subcritical oligomers until their total disappearance (near $t = 6$ s) (Figure 2b):

$$Au_{n,CN^-} + MV^{2+} \rightarrow Au^{+}_{n,CN^-} + MV^{\bullet+} \quad (3)$$

$$Au^{+}_{n,CN^-} \rightarrow Au^{+}{}_{CN^-} + Au_{n-1,CN^-} \quad (4)$$

And eventually

$$Au_{1,CN^-} + MV^{2+} \rightarrow Au^{+}{}_{CN^-} + MV^{\bullet+} \quad (5)$$

According to the coalescence model,[20] the nuclearities of Au_{n,CN^-} in the range 1−2 s are only of a few units. The mechanism of reactions 3−5 implies that the redox potentials of these oligomers of Au_{n,CN^-} are certainly lower than $E°(MV^{2+}/MV^{\bullet+}) = -0.4$ V_{NHE}.

In fact, at long times after γ-irradiation of an identical solution under vacuum, the characteristic $MV^{\bullet+}$ spectrum is obtained alone: as expected, the very first Au_n clusters formed have been oxidized by MV^{2+}, and hence no supercritical cluster may be produced and developed.

Bimetallic $Ag(CN)_2^-$/$Au(CN)_2^-$ Solutions. *Bimetallic Solutions without MV^{2+}.* The bimetallic solutions to be irradiated contain $KAg(CN)_2$ and $KAu(CN)_2$ in a 50/50 ratio. To follow the optical absorption evolution, we selected the same wavelengths as in previous studies on monometallic solutions to facilitate the comparisons, that is at 400 and 520 nm, which correspond to the maximum of the surface plasmon bands of silver and gold clusters, respectively (Figure 3). The early steps of the mechanism are the Ag^I and Au^I reductions with the rate constants 1.5×10^{9} [4] and $(9.5 \pm 1.5) \times 10^9$ L mol^{-1} s^{-1},[13,14] respectively. In an equimolar solution of precursors, complexed gold and silver atoms are thus generated quite readily. Then, within microseconds, the association of these atoms with excess ions may involve the same or different metal species, according to the statistics of the encounters.

$$Au°_{CN^-} + Au^{+}_{CN^-} \rightarrow (Au_2)^{+}_{CN^-} \quad (6)$$

$$Ag°_{CN^-} + Ag^{+}_{CN^-} \rightarrow (Ag_2)^{+}_{CN^-} \quad (7)$$

$$Ag°_{CN^-} + Au^{+}_{CN^-} \rightarrow (AgAu)^{+}_{CN^-} \quad (8)$$

$$Au°_{CN^-} + Ag^{+}_{CN^-} \rightarrow (AgAu)^{+}_{CN^-} \quad (9)$$

The products are identical in reactions 8 and 9.[24] These reactions constitute the early binding between the two metals within the same entity. Mixed species including two different metals have already been detected by pulse radiolysis such as $(TlAg)^+$ in solutions of monovalent−monovalent ions[7] or $(CdAg)^{2+}$ and $(CoAg)^{2+}$ in divalent−monovalent ionic solutions.[8] Further coalescence as in reactions 10 and 11 of the species formed in reactions 8 and 9 would yield alloyed clusters of increasing nuclearity, $(Ag_iAu_j)_{CN^-}$, and thus causes the increase of the extinction coefficient per atom, which accounts for OD increases at 400 and 520 nm at least up to 2 s (Figure 3).

$$(AgAu)^{+}_{CN^-} + (AgAu)^{+}_{CN^-} \rightarrow (Ag_2Au_2)^{2+}_{CN^-} \quad (10)$$

$$(Ag_nAu_m)^{x+}_{CN^-} + (Ag_pAu_q)^{y+}_{CN^-} \rightarrow (Ag_iAu_j)^{z+}_{CN^-} \quad (11)$$

In fact, the total concentration of reduced atoms no longer changes once the scavenging of reducing radicals is complete (<1 μs). The increase at 520 nm is observed only during the first 2 s after the pulse. The increase is much faster than without $Ag(CN)_2^-$. At 2 s, despite the competitive scavenging by Ag^+, the absorbance is almost the same as in pure gold solutions under same dose conditions whereas the 400 nm absorbance is half of that in pure Ag^+ solutions. In fact, if the metal atoms of gold and of silver would coalesce separately and would yield coexisting pure silver clusters and pure gold clusters, the 520 nm absorbance during the first 2s would be less than twice that in pure gold solution, due to the competitive scavenging by Ag^I. These features suggest an interaction between both metal atoms, at least during 2 s, yielding alloyed species, possibly as in (8)−(11).

Beyond 2 s the absorbance increase at 520 nm is followed by a decrease, while OD_{400} continues to increase correlatively. Then the absorbances at 520 and 400 nm reach a plateau at 20 s, the latter being nearly the same as for pure silver solutions, as if the reduction equivalents of gold atoms had been all transferred to silver (Figure 3).

The displacement at long time is confirmed by γ-radiolysis experiments with variable doses (Figure 4). If the dose imparted by γ-irradiation to an equimolar mixed solution ($[Ag^I(CN)_2^-] = [Au^I(CN)_2^-] = 4 \times 10^{-5}$ mol L^{-1}) is lower than 0.25 kGy, so that only partial ion reduction is achieved, the spectrum corresponds to that of almost totally reduced monometallic silver clusters superimposed on the same $Au^I(CN)_2^-$ bands at 232 and 242 nm as before irradiation. Silver is thus clearly reduced first and benefits from electron transfer from transient gold atoms. When the dose is 0.80 kGy, which is sufficient to reduce all the ions of the mixed solution, the spectrum is quite different, and the maximum shifts to 450−470 nm because gold ions are now also reduced at the surface of previously formed silver clusters and the final clusters are composed of a silver core coated by a gold shell.

Therefore, even when formed soon after the pulse, the mixed metal species progressively lose during the coalescence in the

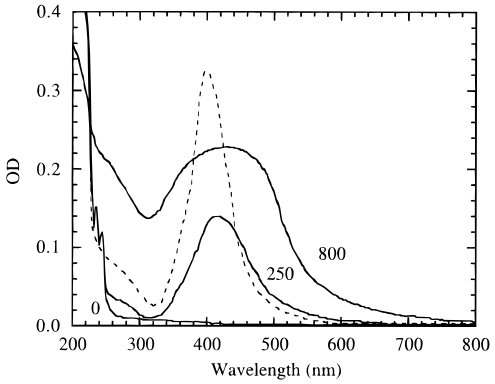

Figure 4. Absorption spectra after γ-irradiation of a mixed solution of silver and gold cyanide (optical path 0.2 cm). $[KAg(CN)_2] = 4 \times 10^{-5}$ mol L^{-1}; $[KAu(CN)_2] = 4 \times 10^{-5}$ mol L^{-1}; $[iPrOH] = 2 \times 10^{-1}$ mol L^{-1}, before irradiation (0), for a 250 Gy dose (partial reduction), and for a 800 Gy dose (total reduction). For comparison, the spectrum of a totally reduced silver solution (- - -) is shown; $[KAg(CN)_2] = 8 \times 10^{-5}$ mol L^{-1}, dose 250 Gy.

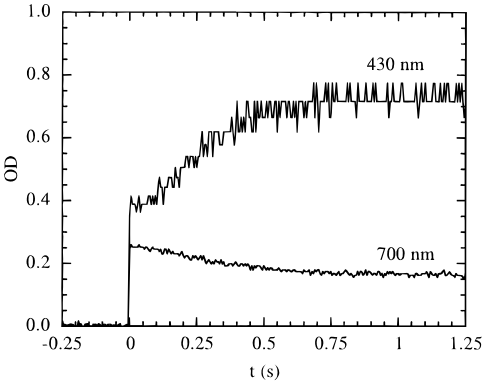

Figure 5. Correlated signals at $\lambda = 700$ nm and $\lambda = 430$ nm with a single pulse in the presence of the electron donor. $[KAg(CN)_2] = 2.5 \times 10^{-4}$ mol L^{-1}; $[KAu(CN)_2] = 2.5 \times 10^{-4}$ mol L^{-1}; $[MV^{2+}] = 5 \times 10^{-4}$ mol L^{-1}; $[iPrOH] = 2 \times 10^{-1}$ mol L^{-1}.

second time range the zero-valent gold and are enriched in silver up to the total disappearance of gold within the clusters: silver ions displace the gold atoms and gold ions are slowly released (reactions 12−14):

$$(Ag_iAu_j)_{CN^-} + Ag^+_{CN^-} \rightarrow (Ag_{i+1}Au_j)^+_{CN^-} \rightarrow (Ag_{i+1}Au_{j-1})_{CN^-} + Au^+_{CN^-} \quad (12)$$

$$(Ag_{i+1}Au_{j-1})_{CN^-} + Ag^+_{CN^-} \rightarrow (Ag_{i+2}Au_j)^+_{CN^-} \rightarrow (Ag_{i+2}Au_{j-2})_{CN^-} + Au^+_{CN^-} \quad (13)$$

$$(Ag_{i+n}Au_{j-n})_{CN^-} + (j-n)Ag^+_{CN^-} \rightarrow (Ag_{i+j})_{CN^-} + (j-n)Au^+_{CN^-} \quad (14)$$

The metals were thus transiently alloyed in each cluster. But eventually, only monometallic silver clusters survive. The gold ions that had scavenged the electrons transfer them back to the silver ions, thus playing the role of a relay. The decrease at 520 nm that occurs at a constant total concentration of metal atoms indicates that at this wavelength the extinction coefficient per atom $\epsilon(Ag_iAu_j)_{CN^-}$ of the bimetallic species present at 1−2 s is almost 2 times greater than $\epsilon(Ag_n)_{CN^-}$ (Figure 3). The correlated increase at 400 nm means that $\epsilon(Ag_iAu_j)_{CN^-}$ is half of $\epsilon(Ag_n)_{CN^-}$ at this wavelength, suggesting that the absorption band of the alloyed cluster is located in the 400−500 nm domain. The progressive replacement of gold atoms by silver atoms in the cluster implies that the redox potential at a given nuclearity is more positive for silver than for gold, which is less noble in the presence of cyanide. Note that the electrode potential of silver cyanide is also more positive (−0.4 V_{NHE}[25]) than that of gold cyanide (−0.6 V_{NHE}[19]). Numerous examples of a similar segregation in mixed core−shell clusters with the more noble metal in the core have already been reported.[5,10,11]

Mixed Solutions of Ag^I/Au^I in the Presence of MV^{2+}. Signals obtained with a mixed solution of Ag^I and Au^I in the presence of the $MV^{2+}/MV^{\bullet+}$ probe will be compared with signals in monometallic solutions (ref 4 and above) with the same redox couple, in order to study the reactivity of the bimetallic clusters. Initial equimolar solutions of metal ions ($[KAu(CN)_2] = [KAg(CN)_2] = 2.5 \times 10^{-4}$ mol l^{-1}) also contained $[MV^{2+}] = 5 \times 10^{-4}$ mol L^{-1}.

After the pulse, the respective initial amounts of metal atoms and of $MV^{\bullet+}$ ions result from the competition between the reduction reactions induced by radiolytic species. If the cluster formed reaches the critical size (as did silver clusters in the preceding study[4]), it will act as a nucleus that initiates a catalyzed growth fed alternatively by the electron donor and the adsorption of excess metal ions. Otherwise, a subcritical cluster is unable to accept an electron from $MV^{\bullet+}$. Moreover the reverse transfer will occur from these clusters to MV^{2+} (faster for gold than for silver[4]).

After a single pulse, the evolution of $MV^{\bullet+}$ is observed at 700 nm and the cluster absorbance at 430 nm, near the minimum of the $MV^{\bullet+}$ spectrum (Figure 5). Actually, the kinetics changes are opposite relative to pure gold solutions, where the oxidation of initial pure gold clusters and the correlated increase of the $MV^{\bullet+}$ signal were observed. The general scheme of $MV^{\bullet+}$ decay now presents the same decreasing features as in the silver case,[4] as if gold in the alloyed cluster exhibited the same properties as silver. We exclude the explanation that gold atoms have already been replaced by silver atoms since the displacement mechanism (12−14) in gold−silver solutions appeared to be much slower ($t > 2$ s) than the process here observed within 20 ms. It is remarkable that after the initial fast increase both the signals of the electron donor $MV^{\bullet+}$ at 700 nm and of the clusters at 430 nm are stable for 10−20 ms: this critical time t_c is that required by clusters to reach the size n_c, having a potential value slightly above that of the monitor. During this time delay, the cluster growth is apparently not affected by the presence of the probe, and the mechanism should be the same as in reactions 6 and 7−11. We observe that the reciprocal of t_c increases linearly with OD_{700} and thus with the initial metal atom concentration, the straight line being the same as in pure silver solutions[4] within the uncertainty of the measurements. The critical time is therefore not affected by the presence of gold ions replacing part of the silver ions in the mixed solution.

We observe that after t_c the absorbance OD_{700} decays while OD_{430} increases, as in silver solutions[4] and in contrast with pure gold solutions. That means that the donor $MV^{\bullet+}$ is consumed catalytically and that subsequent growth of supercritical alloyed clusters occurs (in this time range, the oxidation of subcritical Ag_n or Au_n by the oxidized form MV^{2+} is still negligible).

For $i + j > n_c$,

$$(Ag_iAu_j)^+_{CN^-} + MV^{\bullet+} \rightarrow (Ag_iAu_j)_{CN^-} + MV^{2+} \quad (15)$$

$$(Ag_iAu_j)_{CN^-} + Ag^+_{CN^-} \rightarrow (Ag_{i+1}Au_j)^+_{CN^-} \quad (16)$$

or

$$(Ag_iAu_j)_{CN^-} + Au^+_{CN^-} \rightarrow (Ag_iAu_{j+1})^+_{CN^-} \quad (17)$$

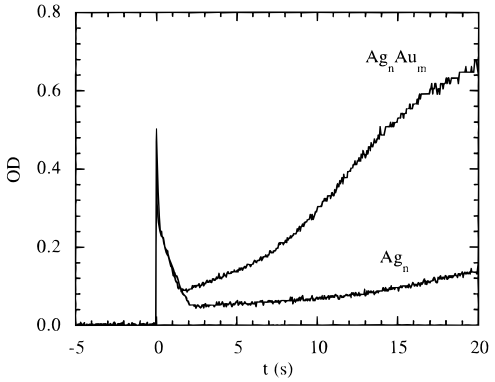

Figure 6. Comparison of signals at $\lambda = 700$ nm in silver cyanide solution and a mixed solution of Ag^I/Au^I (0.50/0.50) having the same total concentration, 5×10^{-4} mol L^{-1}. Above 2 s, $MV^{\bullet+}$ is totally consumed. Dose about twice that in Figure 5.

Then

$$(Ag_{i+1}Au_j)^+_{CN^-} + MV^{\bullet+} \rightarrow (Ag_{i+1}Au_j)_{CN^-} + MV^{2+} \quad (18)$$

or

$$(Ag_iAu_{j+1})^+_{CN^-} + MV^{\bullet+} \rightarrow (Ag_iAu_{j+1})^+_{CN^-} + MV^{2+} \quad (19)$$

In the interval 0.2−2 s we also observe a slower decay than for $t < 0.2$ s which we assign, as previously for silver,[4] to reverse electron transfer from subcritical clusters to MV^{2+} (Figure 5).

For $i+j < n_c$,

$$(Ag_iAu_j)_{CN^-} + MV^{2+} \rightarrow (Ag_iAu_j)^+_{CN^-} + MV^{+} \quad (20)$$

The $MV^{\bullet+}$ formed may transfer back an electron to supercritical clusters (reactions 15, 18, and 19) so that it acts as an electron relay from subcritical to supercritical clusters.[4]

After 2 s the absorbance at 700 nm increases drastically (Figure 6). This absorbance is no longer due to $MV^{\bullet+}$, already consumed, but to the red component of large clusters, which developed from a small concentration of nuclei.[6] The comparison of this signal with that obtained in the case of silver under the same conditions[4] indicates that, when we replace part of the silver ions by gold ions in the solution, the increase of OD_{700}, and therefore that of ϵ_{700} with n, is much greater (twice at 2 s and 5 times at 20 s) for the mixed than for the silver solution (Figure 6) (it was zero for the gold solution). Therefore, a clear synergy is observed in the mixed system, which supports the conclusion of a strong binding between gold and silver atoms and of the bimetallic character of the clusters after the end of the reduction by $MV^{\bullet+}$. Actually, in the presence of methyl viologen, (i) zero-valent gold escapes from complete oxidation by MV^{2+} when it coexists with silver in supercritical clusters, whereas alone it is corroded on the scale of a few seconds; ii) gold atoms included in the alloyed supercritical clusters are not displaced by Ag^+ ions, at least up to 20 s, possibly because the mean cluster size being larger the release of gold ions (reactions 12−14) is much slower; the lifetime of transient alloyed clusters is much longer (at least 40 s instead of 2 s); and (iii) the alloyed clusters developed by $MV^{\bullet+}$ are large due to the competition between MV^{2+} and metal ions, the ions reduced initially being about 2 times less concentrated than without MV^{2+} for the same dose. The reduction equivalent used to form $MV^{\bullet+}$ is then transferred to the initial clusters to let them grow readily without changing their concentration (development process 15−18). The developed gold−silver clusters absorb mostly in the red.

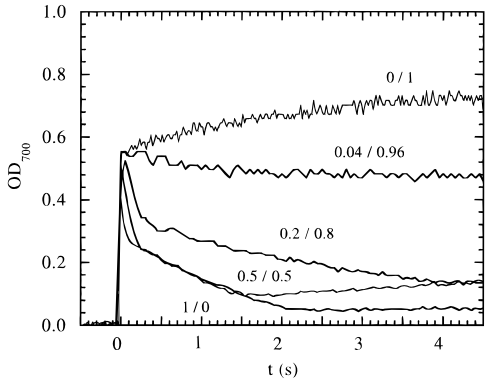

Figure 7. Comparison of long time signals at $\lambda = 700$ nm in silver or gold solution and mixed solutions of Ag^I/Au^I (0.50/0.50), (0.20/0.80), and (0.04/0.96) with pure silver or gold solutions of the same total concentration: $[KAg(CN)_2] + [KAu(CN)_2] = 5 \times 10^{-4}$ mol L^{-1}; $[MV^{2+}] = 5 \times 10^{-4}$ mol L^{-1}; [iPrOH] $= 2 \times 10^{-1}$ mol L^{-1}.

Influence of the Ratio of Gold and Silver Ions in Mixed Solutions. Since the properties of the alloyed cluster $Ag_{0.5}Au_{0.5}$ are strongly dominated by those of silver, it was important to extend the study to ion mixtures much less concentrated in silver. Two other systems containing the ions with ratios of $Ag^I/Au^I = 0.20/0.80$ and 0.04/0.96 were investigated by pulse radiolysis under the same conditions as above. The signals at 700 nm (Figure 7) indicate that the donor decay occurs after a critical time that is nearly the same as that obtained for pure silver or for silver/gold 0.50/0.50 mixed solutions (under equivalent dose conditions). Even with a content in silver ions as low as 0.04/0.96 the absorbance decays for many seconds, in contrast with the pure gold solution, for which an increase of OD_{700} had been observed (Figures 3 and 6). This means that $MV^{\bullet+}$ does not remain as an end product but that electrons are transferred again from $MV^{\bullet+}$ to supercritical clusters. When alloyed with silver atoms shortly after their formation, the gold atoms thus behave differently. The bimetallic cluster exhibits a higher redox potential than pure gold and is developable through alternate reduction by MV^+ and adsorption of Ag^I and Au^I (reactions 16−20).

However, it is clear from comparison between the kinetics in Figure 7 that in the time range of seconds the rate of signal evolution depends markedly on the silver content. It is increasingly slower as the ratio decreases. For all mixed solutions, the final absorbance at 700 nm is greatly enhanced relative to pure silver solutions as a consequence of the red shift of the alloyed cluster spectra.

Redox Potential of Alloyed Clusters. It is noteworthy that, except for the cluster absorbance at long time, the signals are only slightly affected by substitution of an increasing amount of silver ions by gold ions in the initial solution. We conclude that the critical nuclearity for alloyed gold−silver clusters to reach the reference redox potential $E^\circ = -0.4$ V_{NHE} would seemingly be that of pure silver clusters $n_c = 5-6$ in the presence of CN^-,[4] if the coalescence rate constant was not affected by a partial substitution of Ag^I by Au^I. However, due to the much stronger complexation of gold by CN^-, the coalescence of pure reduced species is slower and hence the probability of their reverse corrosion by Ag^I or MV^{2+} is higher. Therefore, $n_c = 5-6$ would be a lower limit for the alloyed cluster if k_d (which could not be evaluated due to the intermetallic electron transfer) was intermediate between the values in the monometallic silver and gold systems. In contrast, when included in alloyed clusters even at a low ratio, silver seems to impose its properties (coalescence rate, redox potential) on the

silver−gold clusters. All these clusters in the presence of cyanide are oxidized by O_2 (−0.33 V_{NHE}).

It is interesting to compare these results with observations on the catalytic efficiency of mass-selected mixed clusters $(Ag_m\text{-}Au_n)^+$ ($m + n = 5$) for the development of photographic emulsions:[26] when $n > m$, no development is observed, in contrast with the case of $n < m$, where the development efficiency is dominated by the silver atom content.

These conclusions are of particularly high interest in the process of gold latensification of silver halide emulsion grains. In the presence of chloride (and in contrast with cyanide), gold atoms exhibit a more noble character than silver atoms in the same cluster of a given nuclearity. Thus, traces of gold ions in the grains favor the trapping of photoelectrons in mixed clusters and fewer silver atoms would be reversely corroded, for instance through electron−hole recombination. This effect is sufficient to enhance the effective quantum yield of atom formation and hence the emulsion sensitivity.

Conclusion

This time-resolved study by pulse radiolysis of mixed solutions of two monovalent metal ions with the same ligand, $Ag(CN)_2^-$ and $Au(CN)_2^-$, has for the first time permitted the observation of the dynamics from the nanosecond to the second ranges of the simultaneous reduction of the ions, then of the atom coalescence, and of the cluster reactivity, and the identification of a transient alloying of both metals. The fast formation of these transient bimetallic clusters is followed by a slow electron transfer in the range 2−20 s from zero-valent gold to silver ions, leading finally to monometallic silver clusters. At a given nuclearity silver clusters are more noble than gold clusters in a cyanide environment. In the presence of the $MV^{2+}/MV^{\bullet+}$ couple the bimetallic clusters accept electrons from $MV^{\bullet+}$ beyond a critical nuclearity, in contrast with monometallic gold clusters, which are oxidized by MV^{2+} and thus are not developed. The redox potential of gold−silver alloyed clusters in cyanide solutions is therefore increased compared to monometallic gold clusters.

Acknowledgment. We are indebted to Dr V. Favaudon of the Curie Institute, Orsay, for access to the Linac facility and to AGFA-GEVAERT Company for financial support.

References and Notes

(1) Bradley, J. S. In *Clusters and Colloids*; Schmid, G., Ed.; Weinheim: New York, 1994; p 459.

(2) Henglein, A. *Chem. Rev.* **1989**, *89*, 1861; *J. Phys.Chem.* **1993**, *97*, 5457.

(3) Belloni, J.; Amblard, J.; Marignier, J. L.; Mostafavi, M. In *Clusters of Atoms and Molecules II*; Haberland, H., Ed.; Chemical Physics: Springer, 1994; Vol. 56, p 291.

(4) de Cointet, C.; Mostafavi, M.; Khatouri, J.; Belloni, J. *J. Phys. Chem. B* **1997**, *101*, 3512.

(5) Belloni, J. *Curr. Opin. Colloid Interface Sci.* **1996**, *1*, 184

(6) Mostafavi M.; Marignier J. L.; Amblard J.; Belloni J. *Radiat. Phys. Chem.* **1989**, *34*, 605; *Z. Phys. D: At. Mol. Clusters* **1989**, *12*, 31.

(7) Ershov, B. G.; Janata, E.; Henglein, A. *J. Phys. Chem.* **1994**, *98*, 10891.

(8) Ershov, B. G.; Janata, E.; Henglein, A. *J. Phys. Chem.* **1994**, *98*, 7619.

(9) Remita H.; Khatouri, J.; Treguer, M.; M.; Amblard, J.; Belloni, J. *Z. Phys. D: At. Mol. Clusters*, in press.

(10) De Cointet, C.; Treguer, M.; Remita H.; Khatouri, J.; Treguer, M.; Mostafavi, M.; Amblard, J.; Belloni, J.; De Keizer, R. *J. Phys. Chem.*, to be published.

(11) Lee, A. F.; Baddeley, C. J.; Hardacre, C.; Ormerod, R. M.; Lambert, R. M.; Schmid, G.; West H. *J. Phys.Chem.* **1995**, *99*, 6096.

(12) Remita, S.; Mostafavi, M.; Delcourt, M. O. *Radiat. Phys. Chem.* **1995**, *47*, 275.

(13) Mosseri, S.; Henglein, A.; Janata, E. *J. Phys. Chem.* **1989**, *93*, 6791.

(14) Gosh-Mazumdar, A. S.; Hart, E. *J. Adv. Chem. Ser.* **1968**, *81*, 193.

(15) Duff, D. G.; Baiker, A.; Edwards, P. P. *Langmuir* **1993**, *9*, 2301.

(16) Siebrands, T.; Giersig, M.; Mulvaney, P.; Fischer Ch.-H. *Langmuir* **1993**, *9*, 2297.

(17) Remita, S.; Archirel, P.; Mostafavi, M. *J. Phys. Chem.* **1995**, *99*, 13198.

(18) Texier, I.; Mostafavi, M. *Radiat. Phys. Chem.*, in press.

(19) Bodlander, G. *Ber. Dtsch. Chem. Ges.* **1903**, *36*, 3933. *Handbook of Chemistry and Physics*, 44th ed.; 1973.

(20) Khatouri, J.; Ridard, J.; Mostafavi, M.; Amblard, J.; Belloni, J. *Z. Phys. D: At. Mol. Clusters* **1995**, *34*, 57.

(21) Latimer, W. M. *Oxidation Potentials*, 2nd ed.; Prentice-Hall: Englewood Cliffs, NJ, 1952.

(22) Azzam, A. M.; Shimi, I. A. W. *Z. Anorg. Chem.* **1963**, *321*, 284**.**

(23) Mostafavi, M.; Delcourt, M. O.; Belloni, J. *J. Imaging Sci.* **1994**, *38*, 54.

(24) Belloni, J.; Delcourt, M. O.; Marignier, J. L.; Amblard, J. In *Radiation Chemistry*; Hedwig, P., Nyikos, L., Schiller, R., Eds.; Akademiaï Kiado: Budapest, 1987; p 89.

(25) Gauguin, R. *J. Chim. Phys.* **1945**, *42*, 28.

(26) Rosche, C.; Wolf, S.; Leisner, T.; Granzer, F.; Wöste, L. *Proc. IS&T's 48th Annu. Conf.*, Washington, DC, **1995**, p 325.